INTERNATIONAL JOURNAL OF CLIMATOLOGY
Int. J. Climatol. (2015)
Published online in Wiley Online Library
(wileyonlinelibrary.com) DOI: 10.1002/joc.4274

RMetS
Royal Meteorological Society

An estimation of the land-atmosphere coupling strength in South America using the Global Land Data Assimilation System

Pablo C. Spennemann[a]* and Andrea Celeste Saulo[a,b]

[a] *Centro de Investigaciones del Mar y la Atmósfera (CONICET-UBA), UMI IFAECI/CNRS, Buenos Aires, Argentina*
[b] *Departamento de Ciencias de la Atmósfera y los Océanos, Facultad de Ciencias Exactas y Naturales, Universidad de Buenos Aires, Argentina*

ABSTRACT: The aim of this study is to identify regions of strong land surface–atmosphere coupling for the austral summer over South America. To accomplish this, a statistical methodology is applied to estimate the interactions of soil moisture with evapotranspiration and precipitation derived from the Global Land Data Assimilation System (GLDAS) dataset. Possible impacts of El Niño Southern Oscillation (ENSO) on the coupling strength are also examined. Particular emphasis is set over two sub-regions of interest: Southeastern South America (SESA) and the continental part of the South Atlantic Convergence Zone (SACZ). Positive and significant soil moisture–precipitation feedbacks are found over parts of SACZ and in the southern part of South America. Instead, significant negative feedback is found over SESA. The influence of ENSO over the soil moisture–precipitation coupling strength signal is evident over tropical regions. Plausible physical mechanisms involved in the land surface–atmosphere interactions, the influence of ENSO and that of precipitation persistence over extratropical regions on the results, are discussed. The implications of this analysis on monthly to seasonal forecast are also examined. Despite that this methodology cannot be used to establish a precise causal–effect relationship, this study gives a valuable first order approximation of land surface–atmosphere interactions over South America that complements pre-existing work.

KEY WORDS land surface–atmosphere interactions; soil moisture; precipitation; South America; GLDAS

Received 16 July 2013; Revised 23 December 2014; Accepted 12 January 2015

1. Introduction

Many papers document the importance of soil moisture in modulating atmospheric variability at various time scales ranging from synoptic to seasonal. The underlying hypothesis is that soil moisture variability is much slower than that of atmospheric variables, and thus controls atmospheric conditions through different coupling mechanisms. The degree of control (i.e. coupling strength) that soil moisture anomalies can exert on climate is highly variable, and is stronger over transitional regions between dry and wet climates and where soil moisture memory is longer (Seneviratne *et al.*, 2010).

Land–atmosphere coupling strength has been mainly analysed using model simulations and model intercomparisons (Koster *et al.*, 2002, 2004; among others). The Global Land-Atmosphere Coupling Experiment (GLACE, Koster *et al.*, 2006) is probably the most important effort to document the land-atmosphere coupling strength and its uncertainty during the boreal summer. Given the relatively expensive computational cost of GLACE at that time, this experiment has been run only for one summer season using 12 different models with 16 ensemble members and the same sea surface temperature (SST) field corresponding to neutral El Niño Southern Oscillation (ENSO) conditions for all the ensemble members. As noted by Seneviratne *et al.* (2006) and Notaro (2008) this may constrain the statistical robustness of the conclusions driven in that assessment. Unfortunately, neither GLACE nor GLACE-2 Koster *et al.*, (2010), study the austral summer. Applying the same methodology as in GLACE, Sörensson *et al.* (2010) analyse the coupling strength with one regional climate model over South America from November 1992 to March 1993, that corresponds to neutral ENSO conditions. This work shows significant month to month variability of the areas where soil moisture exerts some control on precipitation and on evapotranspiration. More recently, Sun and Wang (2012) perform a set of sensitivity experiments to analyse coupling strength, including the austral summer. Their work shows that almost none of the areas with strong coupling in the control run remain after removing the low frequency variations due to SST in the idealized run.

On the other hand, only few studies use *in situ* observations (e.g. Betts *et al.*, 1996, Salvucci *et al.*, 2002, Betts, 2009), mainly due to the scarcity of soil moisture measurements worldwide. This limitation is even more severe in some regions, such as South America and Africa. In turn, remote-sensing derived estimates are still not adequate to perform long term analysis (see Seneviratne *et al.* (2010) for a review on different data sets and their pros and cons).

* Correspondence to: P. C. Spennemann, Ciudad Universitaria, 2do, piso Pabellón II, Buenos Aires, Argentina. E-mail: pspennemann@cima.fcen.uba.ar

Nevertheless, the use of observational based datasets combined with numerical models, such as off-line simulations and reanalysis (Rodell *et al.*, 2004, Dirmeyer, 2011; Mei and Wang, 2012; among others) has increased in the past years. Dirmeyer (2011) highlights possible drawbacks of using reanalysis (e.g. Modern-Era Retrospective Analysis (MERRA)-Land) for long term representation of the hydrological cycle, due to the ingestion of non-stationary satellite data. The author concludes that for assessing soil moisture–evapotranspiration interactions, off-line simulations produce more consistent results. Under this scenario, off-line simulations using land surface models (LSMs) forced with a combination of reanalysis and observed atmospheric variables (hence avoiding the effect of atmospheric model biases), become valuable alternatives to study some aspects of the land–surface interactions. Among this group of observational driven simulation datasets, we can list the Global Soil Wetness Project, version 2 (GSWP-2, Dirmeyer *et al.*, 2006), the Global Offline Land-surface Dataset version 2 (GOLD-2, Dirmeyer and Tan, 2001), the Water and Global Change Project (WATCH, Weedon *et al.*, 2011) and the Global Land Data Assimilation System (GLDAS versions 1 and 2, Rodell *et al.*, 2004). In particular, GLDAS and WATCH use several LSM and comprise longer periods compared with GSWP-2 and GOLD-2 datasets. A relevant issue regarding these data sets is the strong sensitivity of the land surface variables, and hence of the results, to the LSM used for their estimation (e.g. Koster *et al.*, 2004; Guo *et al.*, 2006; Koster *et al.*, 2006 and Zhang *et al.*, 2011). As clearly discussed by Koster *et al.* (2009), the model's soil moisture values are to be thought of as model dependent indices and not as actual soil water content. In this sense it must be kept in mind that any result involving a specific LSM may not be representative of other LSMs and/or of the actual observations.

To assess soil moisture–precipitation/evapotranspiration coupling strength, different statistical approaches have been applied (e.g. Zeng *et al.*, 2010; Dirmeyer, 2011, Mei and Wang, 2012). Some of these methodologies were designed to analyse short time scale interactions (using daily values) and others focus on longer time interactions. For example, using daily soil moisture and precipitation values from reanalysis and offline simulations, Mei and Wang (2012) assess the summer coupling strength over the United States, calculating the probability density function of conditioned correlation between soil moisture and subsequent precipitation. Zhang *et al.* (2008) – hereafter Z08 – apply a statistical approach (originally proposed by Frankignoul and Hasselmann, 1977) on a monthly basis to assess the soil moisture–precipitation coupling strength for the boreal summer using GLDAS-1 and the Climate Prediction Center (CPC) Merged Analysis of Precipitation (CMAP) precipitation data. This work uses three different LSM to perform the assessment and find no significant differences in the sign and/or the pattern of the coupling strength. One limitation of these statistical approaches is that remote forcing effects (e.g. the role of SST on precipitation over land) have to be removed or treated in a specific way to avoid misinterpretation of the results. In order to minimize the SST influence on precipitation, Z08 apply their analysis to a subset of years without ENSO and they conclude that outside tropical regions, their results are robust and coherent with those obtained in GLACE. Although Notaro (2008) and Dirmeyer (2011) claim to find similar results to GLACE regarding the location of the so-called hot spots, a detailed analysis during the austral summer over South America reveals differences among them that might be due to ENSO effects which are not explicitly removed in any of these works. Also, Orlowsky and Seneviratne (2010) – hereafter OS10 – apply the same statistical approach as Z08 to analyse the effect of soil moisture and SST on precipitation and temperature, to discuss the relative contribution of remote versus local influences. One important argument introduced in OS10 is that soil moisture–precipitation coupling strength could be strongly controlled by SST interactions with both variables, thus leading to incorrect conclusions regarding causality. OS10 conclude that most areas of strong soil moisture–precipitation coupling are also areas where SST-precipitation coupling is strong. These results suggest that inferences about soil moisture control on precipitation should be done carefully over those regions. One drawback of OS10 compared with Z08, is that they use the precipitation from the European Centre for Medium-Range Weather Forecasts (ECMWF) reanalysis (ERA-40, Uppala *et al.*, 2005), instead of using an observational precipitation dataset. Their study also focuses only on the boreal summer. Sun and Wang (2012) examine this statistical methodology applied to climate model outputs over North America, and point out that in order to represent more precisely the coupling strength, soil moisture should have a much longer memory than the atmospheric memory, which is not the case, for instance, in tropical regions (Dirmeyer *et al.*, 2009).

Considering that over South America, GLDAS-2 precipitation variability is more representative of *in situ* observed precipitation variability at monthly time scales than at daily ones, we propose to analyse soil moisture–precipitation coupling strength at monthly time scales applying a methodology similar to Z08 over South America during the austral summer. Our focus will be in central and southern South America, outside the tropics, where this methodology is more reliable according to previous studies. To improve the robustness of the calculations, we employ GLDAS-2 instead of GLDAS-1, because GLDAS-1 forcing fields variability may not be appropriate to perform long term analysis (Rui, 2012). This choice of also implies that our results are dependent on the representativeness and quality of the NOAH LSM used for GLDAS-2 generation. Still, data set stability in terms of its statistical properties is of main concern for our purpose. Our underlying assumption, that the NOAH LSM provides a physically consistent land surface data base, is supported by several studies (e.g. Xia *et al.*, 2013) some of which have focused over South America (Lee and Berbery, 2012; Müller *et al.*, 2014). However, a brief assessment of inter-LSM uncertainty – calculated using

GLDAS-1 – and its impact on coupling strength has been added in the Appendix.

Z08 approach shares with Notaro (2008) and OS10 the same statistical method but handles the plausible effect of SST remote forcing on precipitation by assuming that ENSO is the main source of this effect. In this sense, the analysis of years with and without ENSO is the basis to distinguish, at least as a first order approximation, remote versus local influences. The effect of ENSO on precipitation over distinct regions in South America is supported by several investigations (see Vera *et al.*, 2006 and Marengo *et al.*, 2012 for a review on this topic). According to them, precipitation variance in summer is mostly explained by synoptic and intraseasonal variability, whereas at longer time scales the ENSO is recognized as the most clear remote forcing on precipitation (e.g. Zhou and Lau, 2001; Nogués-Paegle and Mo, 2002). Still, it should be noted that there remain important portions of variability at seasonal and longer time scales that cannot be linked to a specific driving mechanism.

It is important to remark here that, using monthly values entails to lose some relevant shorter scale coupling strength signal and that, despite of the statistical approach used to quantify the coupling strength; none of them ensures causality between the variables.

This work also includes a soil moisture–evapotranspiration coupling strength and simultaneous evapotranspiration–temperature correlation analysis. They are aimed at providing other hints to evaluate possible pathways for land–atmospheric interactions. It is expected that this work will aid in documenting the degree of land–atmosphere coupling at monthly timescales over South America, and hence contribute to provide alternative tools for improved seasonal forecasts in the region.

This work is structured as follows: Section 2 describes data and methodology, Section 3 presents the results and the main conclusions including a brief discussion are provided in Section 4.

2. Data and methodology

In this work we use precipitation, soil moisture and evapotranspiration fields from GLDAS. This project includes several alternatives to construct various surface data sets using four different LSMs driven by diverse atmospheric data, including analysed and observed fields such as radiation and precipitation. Global data sets of soil moisture and other surface variables obtained from long term off-line runs with the different LSMs are also available through GLDAS. In particular, the version 2 of GLDAS, has been generated using the NOAH LSM (Chen *et al.*, 1996; Ek *et al.*, 2003) forced by the global meteorological forcing data set from Princeton University (Sheffield *et al.*, 2006). This array of atmospheric data is a combination of various sources of information including observed precipitation: CRU (TS2.0, 1948–2000, Mitchell and Jones 2005), GPCP (1997–2008, Huffman *et al.*, 2001), TRMM (2002–2008, Huffman *et al.*, 2003), observed short and long wave radiation (NASA Langley SRB, 1983–1995, Stackhouse *et al.*, 2004) and the NCEP-NCAR reanalysis (Kalnay *et al.*, 1996). The main improvement in Version 2 is that a climatologically more consistent dataset is used to force the NOAH LSM, extending from 1948 to 2008. In Version 1, forcing sources switched several times throughout the record from 1979 to till date, which introduced unnatural trends and exhibited highly uncertain forcing fields in 1995–1997 (Rui, 2012).

It is important to highlight that, as mentioned earlier, deficiencies in LSM parameterizations are also sources of errors. In fact, there can be important differences in simulated soil moisture/evaporation between LSMs of similar complexity, as documented in Guo *et al.* (2006), Kato *et al.* (2007) and Xia *et al.* (2014). Thus, a decision had to be made whether to use GLDAS-1 or GLDAS-2. GLDAS-1 allows the analysis of LSM uncertainty but is affected by lack of consistency in the forcing dataset, while GLDAS-2, represents the behaviour of only one LSM, but with is more reliable in statistical terms. In this sense, analysing the inter-LSM uncertainties, Kato *et al.* (2007) observed differences of 25% in soil moisture and 13–113% in seasonal evapotranspiration over four sites of the Coordinated Enhanced Observing Period (CEOP) for 2002–2003. Analysing the impacts of different precipitation datasets on the simulations of a LSM for 1 year (2002–2003), Gottschalck *et al.* (2005) document differences in the total soil moisture content ranging from −75% to 100% over the United States. In addition, Zaitchik *et al.* (2010) using GLDAS-1 and GLDAS-2 LSM, testing a routing scheme for estimating the river discharge around the world conclude that despite the inter-LSM differences, the best results were achieved with GLDAS-2. It should be noted, however, that our work does not focus on actual soil moisture/evaporation amounts, but on the relationship between these variables. In this sense, Z08 do not find significant differences in the correlations, the feedback parameter and or percentage of variance explained while comparing different LSM. Hence, in this study we decided to use $1^\circ \times 1^\circ$ gridded monthly means of GLDAS-2 (identified as 2.7.1, GLDAS/NOAH experiment 001) from November to February for the period 1980–2008, covering South America. We use this subset instead of the whole period available because the atmospheric forcing, based on the NCEP reanalysis, is more reliable when more satellite information is ingested into the assimilation system, particularly over data scarce areas as South America. Despite that GLDAS-1 forcing datasets present some disadvantages, a discussion about the inter-LSMs uncertainties is presented in the Appendix.

The anomalies are computed removing the annual cycle and the interannual trend, and normalized in order to compare our results with other works. A spatial smoothing using a 3-point filter in latitude and longitude is applied, motivated by the idea of representing a more non-local soil moisture-precipitation feedback, as in Z08. In order to retain the memory originating from deep layers, as in OS10, the total depth absolute soil water content (0–200 cm, in $\mathrm{kg\,m^{-2}}$) referred to as soil moisture, is employed. Tests performed using different depths (i.e.

10–100 cm) do not show significant differences with the results presented here.

Coupling strength is calculated here using a simple statistical methodology originally proposed by Frankignoul and Hasselmann (1977) that was later adapted to study the interaction between the atmosphere and ocean sensible heat fluxes (e.g. Frankignoul *et al.*, 1998; Czaja and Frankignoul, 2002). More recently it was applied to the analysis of coupling between vegetation/soil moisture/SST and precipitation (Liu *et al.*, 2006; Notaro *et al.*, 2006; Z08; Notaro, 2008; OS10; Sun and Wang, 2012). Essentially, this approach assumes a linear relationship between two variables, where a slowly varying variable (e.g. soil moisture, S) acts on a faster variable (e.g. precipitation, P) at time $t + \mathrm{d}t$ and is expressed as:

$$P(t + \mathrm{d}t) = \lambda_p S(t) + N(t + \mathrm{d}t) \quad (1)$$

where $N(t+dt)$ represents the internal variability of the atmosphere (or noise) and λ_p is called the feedback parameter. Taking the covariance of both sides with $S(t-\tau)$, where $T > dt$, it follows that:

$$\lambda_{\mathrm{p}} = \mathrm{Cov}\left(S(t - \tau), P(t)\right) / \mathrm{Cov}(S(t - \tau), S(t)) \quad (2)$$

where the covariance between $S(t-\tau)$ and $N(t+\tau)$ is set equal to 0, which is reasonable for $\tau = 1$ month. Thus, λ_p measures the instantaneous (in our case within a month) feedback of S on P at time t. It should be noted that when expression (2) is applied to normalized variables, then λ_p represents the ratio between lagged correlations. Also, provided that we are using a data set from an uncoupled system (the atmosphere is forcing the LSM, but the other way round is not guaranteed) it should be kept in mind that 'the soil moisture feedback on precipitation could only be inferred by studying its covariability when the soil moisture is leading' as clearly stated by Z08. As any covariability measure, it is important to note that large λ_p does not imply causal relation between S and P (see OS10 for a comprehensive discussion of possible physical linkages that may lead to large values of λ_p). Moreover, in order to relate P with S, it is important to minimize other influences (e.g. that of SST on P and or S) that may act on monthly time scales. To account for this, and following Z08, we calculate λ_p removing ENSO years, as a first order approach to minimize remote SST influence on local precipitation during the austral summer. Consequently, for our period of study, the following summer periods have been subtracted: 1982–1983, 1987–1988, 1988–1989, 1991–1992, 1997–1998, 1998–1999, 1999–2000, 2000–2001, 2002–2003, 2004–2005, according to the CPC definition of ENSO years (http://www.cpc.ncep.noaa.gov/products/analysis_monitoring/ensostuff/ensoyears.shtml). After this, our sample has been reduced from 87 to 57 summer months. However, we also present the comparison between periods with and without ENSO years, to further understand the impact of the proposed methodology on the results.

A bootstrap technique (von Storch and Zwiers, 1999) has been applied to evaluate the statistical significance of λ_p. Following OS10, for each grid cell, 1000 iterations are computed keeping soil moisture series invariant and shuffling precipitation series. This way of using the bootstrap technique maintains the information of soil moisture memory and is adequate to simulate the null hypothesis of no relation between both variables. A similar procedure has been used to analyse the feedback parameter between soil moisture and evapotranspiration (denoted here as λ_{evap}). The original feedback parameter is then compared against the 'bootstrap' sample and if the probability is higher than 95% (for $\lambda_p > 0$) or lower than 5% ($\lambda_p < 0$) we say it is significant.

Of particular interest for us are the results over two sub-regions (see Figure 1): the southeastern part of South America (SESA, 35–25°S latitude and 63–50°W longitude) and the continental part of the South Atlantic Convergence Zone (SACZ, 25–15°S latitude and 54–45°W longitude). Our interest follows from many studies documenting the importance of precipitation variability at intraseasonal scales over these regions (see Vera *et al.*, 2006 for a review on this topic), the significant response to ENSO signal – particularly over SESA – and the question regarding how much precipitation variability can be ascribed to local versus remote forcing.

The schematic in Figure 2(a) and (b) introduces the conceptual framework widely adopted to discuss the main land–atmosphere interactions (e.g. Seneviratne *et al.*, 2010), emphasizing the variables and processes analysed in this work. In this diagram, we are assuming that the interactions occur within the same month, i.e. they are instantaneous. The interaction of precipitation with soil moisture is, naturally, positively correlated. However, the interaction of soil moisture with precipitation (e.g. the way back of the loop) does not always have the same sign, because it depends on which process controls evapotranspiration from the surface. One possible pathway is drawn in Figure 2(a), where evapotranspiration is 'controlled' by surface water, meaning that, regardless the amount of radiation, evaporation will be regulated by soil moisture availability. This is usually referred to as 'land control' regime (Seneviratne *et al.*, 2010; Dirmeyer, 2011), and generally leads to a positive feedback between soil moisture and precipitation (enhanced precipitation, enhanced soil moisture, enhanced evapotranspiration, enhanced precipitation). Negative correlations (e.g. less precipitation with more soil moisture) may also appear in a land control regime as a response to weaker atmospheric instability associated to evaporative cooling near the surface (not considered in the diagram). Another pathway is when evapotranspiration is limited by 'energy' (Figure 2(b)), implying that the soil is wet enough and the surface evaporates in response to radiative heating; soil moisture does not control the amount of evapotranspiration. This situation is also referred to as 'atmospheric control.' In this case negative instantaneous correlation between soil moisture, evapotranspiration and consequently precipitation may occur (e.g. increased soil moisture, decreased evapotranspiration, as a response to decreased temperature, and less precipitation), as indicated by the 'NC'

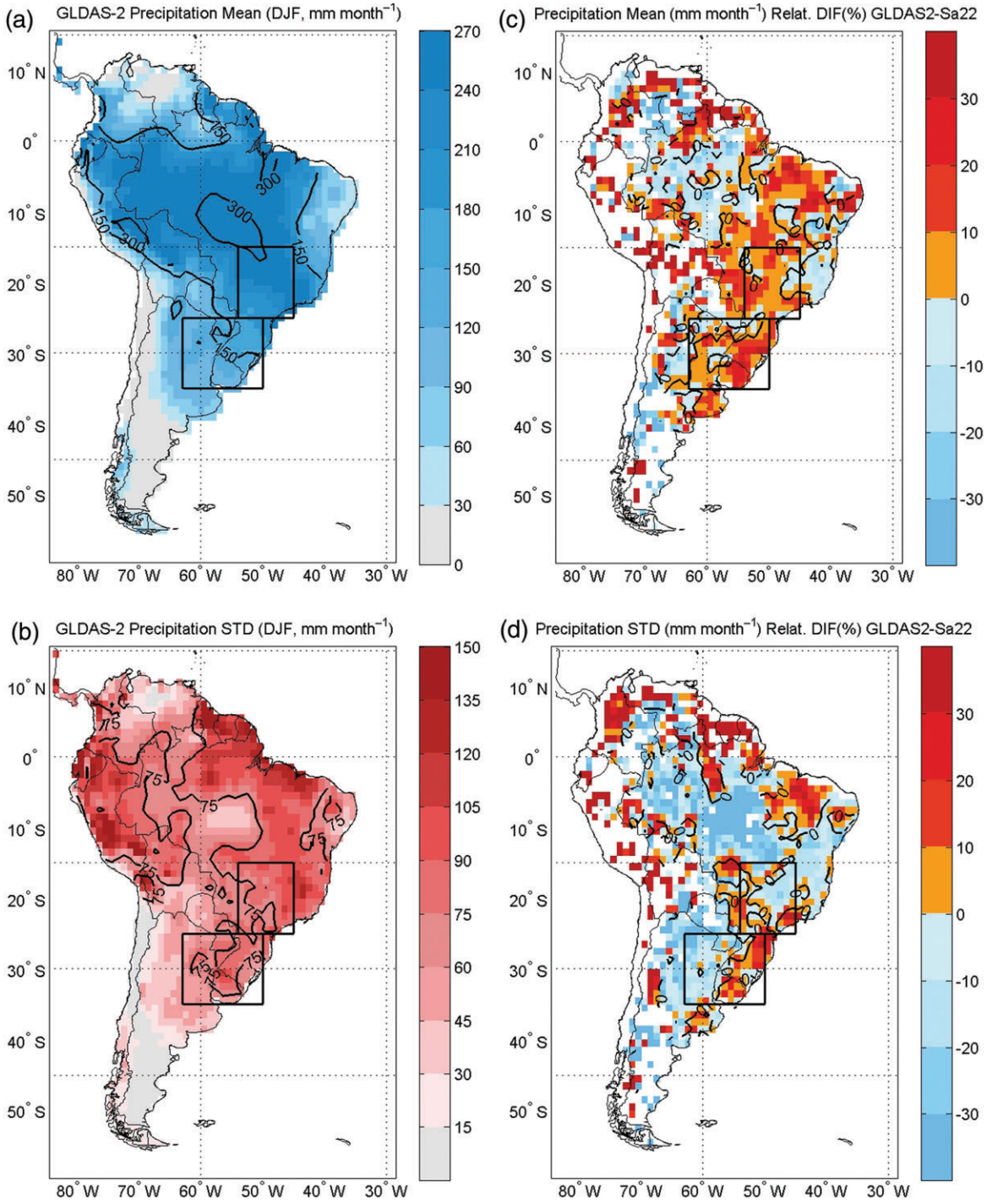

Figure 1. GLDAS-2 summer (DJF) mean precipitation (mm month^{-1}, a), standard deviation (b) and the corresponding relative differences (%, c and d), compared with Sa22. The boxes are used to highlight sub-regions of interest. White grid-boxes in the right panel correspond to areas where Sa22 has no data.

pathway. Under an atmospheric control regime, there can also be positive correlations thus creating a positive feedback between precipitation and soil moisture ('PC' pathway).

Last, it is convenient to highlight what we consider are the main limitations of the dataset and the methodology selected to perform this analysis. The GLDAS-2 is essentially a model driven data set and as such, it will be affected by the NOAH LSM biases. Despite this, the NOAH has been widely validated and evaluated in previous studies (e.g. Sridhar *et al.*, 2003; Schaake *et al.*, 2004; Guo and Dirmeyer, 2006; Kato *et al.*, 2007; Livneh *et al.*, 2010, Jaksa *et al.*, 2013; Xia *et al.*, 2013), including some focusing in South America (Lee and Berbery, 2012, Müller *et al.*, 2014). Regarding the statistical methodology, it is clear that large correlation/covariance between two variables will not explain causality. Moreover the role of a third variable (e.g. SST) on either one or on

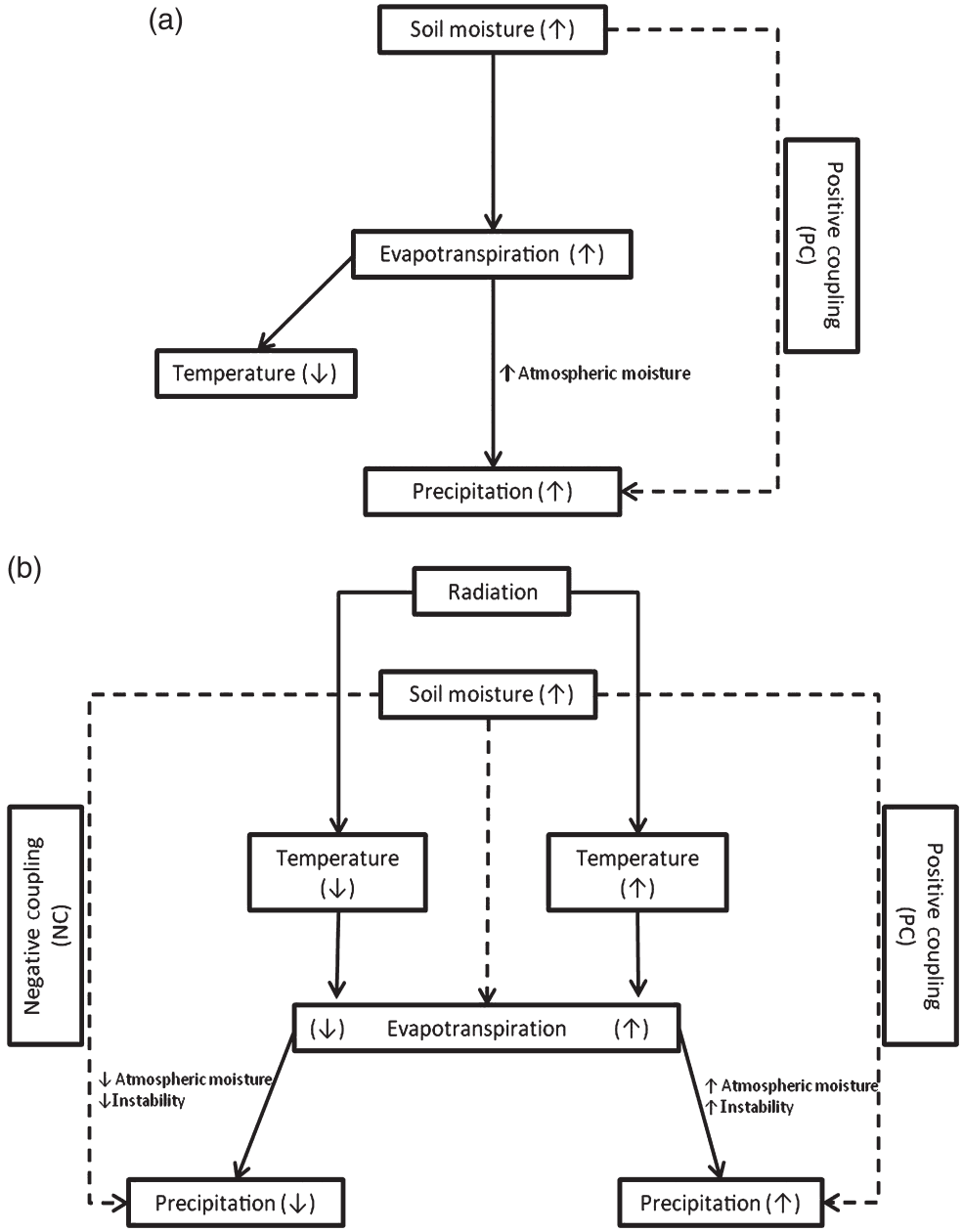

Figure 2. Diagram of the most common interactions among different variables under a land control regime (a) and an atmospheric control one (b). Small arrows (↑, ↓) indicate increase or decrease of each variable. See text for more detail.

both could be responsible for these large correlations. Still, we consider that there is useful information that can be derived from the proposed analysis if its limitations are handled properly. According to the state of the art, alternate ways to analyse land–atmosphere interactions, including their physical explanation, are still in debate and certainly need more research.

3. Results

3.1. Estimation of land surface–atmosphere coupling strength

Precipitation amounts and their temporal variability are critical inputs for any LSM. In order to validate GLDAS-2 seasonal mean (DJF) precipitation and its standard deviation with respect to the 1980–2008 climatological mean, Figure 1 includes a comparison between an observational data set (referred to as Sa22, Liebmann and Allured, 2005) and GLDAS-2. Besides spots with large discrepancies, that mainly occur over areas of complex topography and in tropical regions, precipitation amounts in both data sets are similar, with differences in the mean field below 20% over most of the areas, and somewhat larger in variability (but below 30%). Unfortunately, there are areas without observational data coverage (e.g. southern Argentina) were GLDAS-2 precipitation values cannot be validated. In general, mean values tend to be overestimated by GLDAS-2 and the standard deviation underestimated. The agreement between datasets provides further confidence

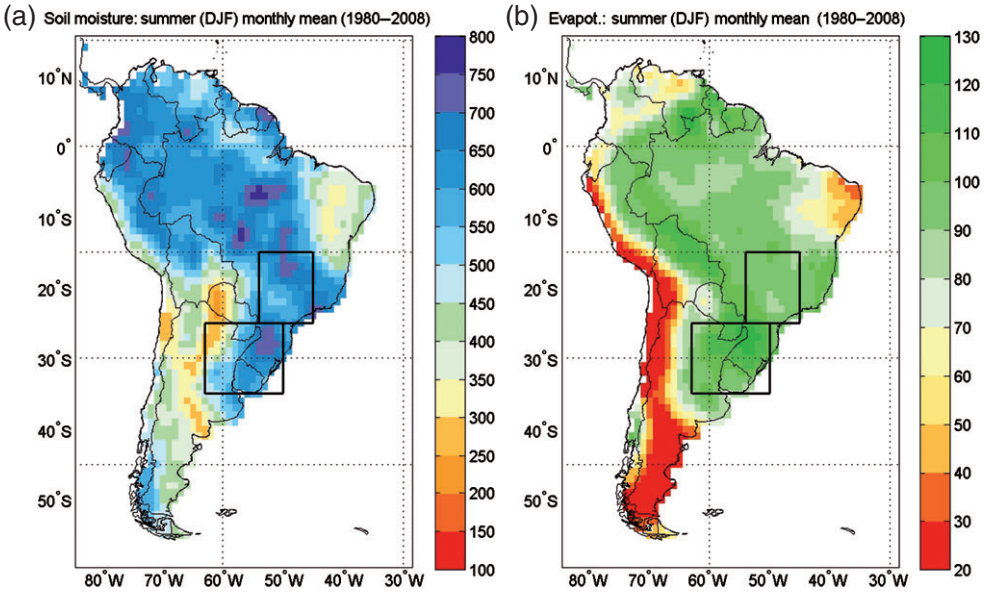

Figure 3. GLDAS-2 summer (DJF) mean soil moisture (kg m^{-2}, a) and evapotranspiration (mm month^{-1}, b).

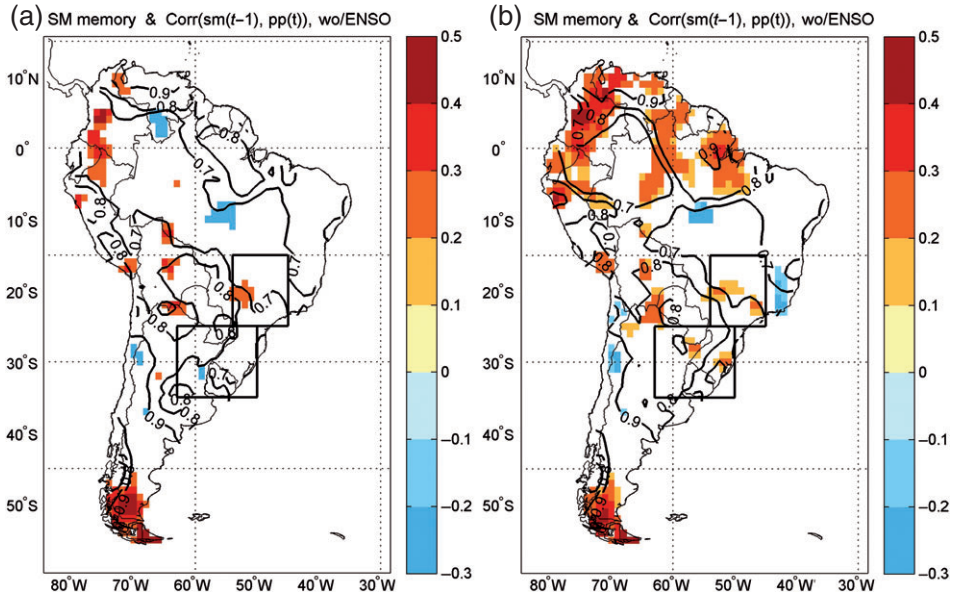

Figure 4. Correlation between monthly mean soil moisture (NDJ) and precipitation (DJF) anomalies (at 90% confidence level, shaded), and soil moisture autocorrelation (lag 1 month, in contours). (a) Sample without ENSO summers. (b) Sample with ENSO summers.

on the representativeness of GLDAS-2 fields to undertake this research at least over relatively flat areas and over the sub-regions of interest.

Mean December–January–February (DJF) soil moisture and evaporation are shown in Figure 3, to illustrate their spatial pattern. As expected, soil moisture closely resembles the precipitation geographical distribution, with maximum values over the Amazon region, the continental portion of the SACZ and parts of Southeastern South America (SESA). In turn, maximum evapotranspiration occurs over SESA and northern Brazil-southern Venezuela. Evapotranspiration variability represented by the standard deviation, shows also maximum values in SESA (not shown). Important horizontal W–E gradients in both mean fields are evident across Argentina and in northeastern Brazil. These areas represent the main transitional zones between dry and wet climates in South America.

A first indication of soil moisture memory is given by the lag 1 autocorrelation (hereafter we will consider equivalent: lag 1 autocorrelation, memory and persistence), which is shown in Figure 4 together with the lagged correlation between soil moisture and precipitation anomalies (soil moisture leading) for periods with and without ENSO years. In both cases soil moisture memory is large, with the lowest lag 1 autocorrelation values (~0.7) in Central Amazon. Contrastingly, lagged correlation between soil moisture and precipitation anomalies changes between both samples: few areas exhibit significant correlations if ENSO

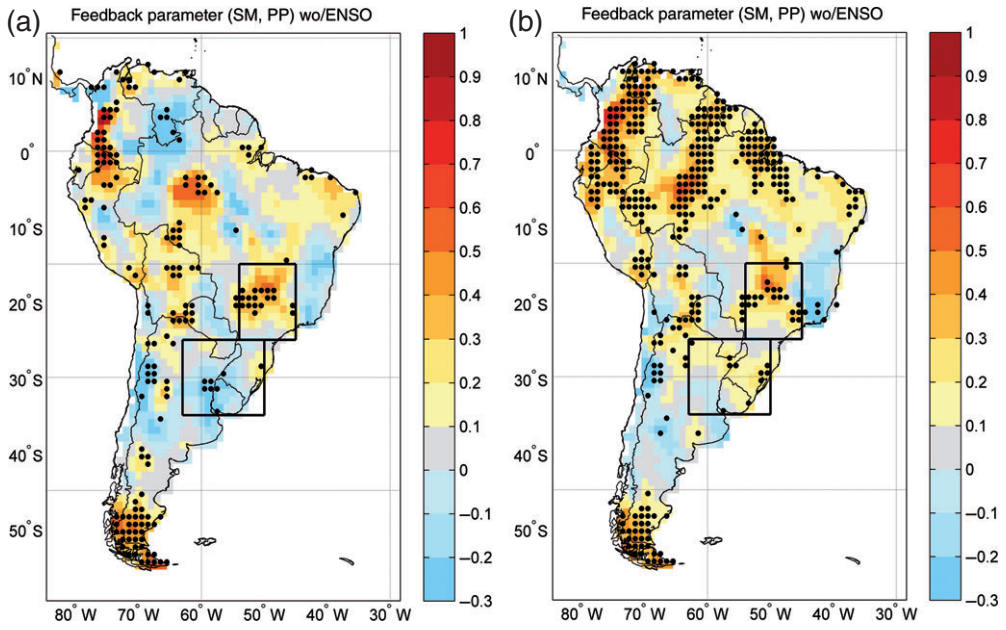

Figure 5. Feedback parameter (λ_p, DJF) for normalized soil moisture-precipitation, without ENSO summers (a), and including ENSO summers (b). Grid points above 90% confidence level are marked with black dots.

years are removed while larger areas appear when ENSO years are included, particularly over tropical regions. In general these correlations are positive. Potential pathways for soil moisture–precipitation and SST interactions are explained in detail by OS10 and Seneviratne *et al.* (2010). Clearly, it is not possible to distinguish between the two physical coupling mechanisms proposed above just using a statistical approach as in here. It is also clear that the strongest influence of ENSO is over tropical areas, which is in agreement with Z08 and Sun and Wang (2012) results. Areas with longer memory and high correlation (without ENSO) outside the tropics mainly occur in the southern tip of the continent (memory > 0.9) and in sparse small areas. These areas also appear in the complete sample. Regarding the area in southern Argentina and Chile, it is characterized by marked W–E rain gradients, with relatively large precipitation amounts to the west, and soil moisture values as large as those over eastern Argentina. This is the most regionally coherent area with maximum of land–atmosphere interaction apparently unaffected by remote influences in our domain of study. Zeng *et al.* (2010) and Sun and Wang (2012) using different methodologies also found a 'hot spot' over southern South America, but maximizing further north.

The feedback parameter is a synthesis of the previous fields, because it is essentially the ratio between 1-month lagged soil moisture–precipitation correlations and 1-month lagged soil moisture autocorrelation (see Equation (2)). The results for both samples are shown in Figure 5. There are obvious similarities with Figure 4, but areas with significant negative coupling between soil moisture and precipitation during non-ENSO years, which are not apparent in ENSO years, become clearer. Moreover, in some regions, the sign of the feedback parameter reverses between the two samples (e.g. over eastern Argentina, parts of southern Brazil and Uruguay, and in the limit between Brazil, Venezuela and the Guyana's), suggesting that it is difficult to drive conclusive results from this diagnostic. Comparing our results with OS10, even considering that their analysis corresponds to June–July–August (JJA), there are some coincidences: spotty areas between the Equator and 20°S with significant positive coupling values, not necessarily related to SST, and the increased coupling strength in tropical areas when ENSO years are included, which in OS10 correspond to areas where both coupling strengths (soil moisture/precipitation and SST/precipitation) are important. It should be noted that OS10 compare SST-precipitation with soil moisture–precipitation coupling strengths, searching for regions where the coupling is strong for each variable individually and for both at the same time. In the latter case, no conclusions can be made concerning which variable is locally influencing the precipitation. Thus, they do not isolate the effects of any of these forcings. Our approach is different in the sense that for non-ENSO years, we are assuming that on monthly time scales, precipitation is a result of internal variability and soil moisture related effects only, as evidenced by Equation (1).

The negative sign in λ_p is not easy to interpret but there are other studies showing this over different regions (e.g. Z08; OS10; Dirmeyer, 2011; Sun and Wang, 2012). We will propose an explanation after including the role of evapotranspiration using the conceptual framework synthesized in Figure 2.

3.2. Possible mechanisms underlying land–atmosphere coupling

In order to analyse possible pathways for soil moisture–precipitation interaction we document the coupling

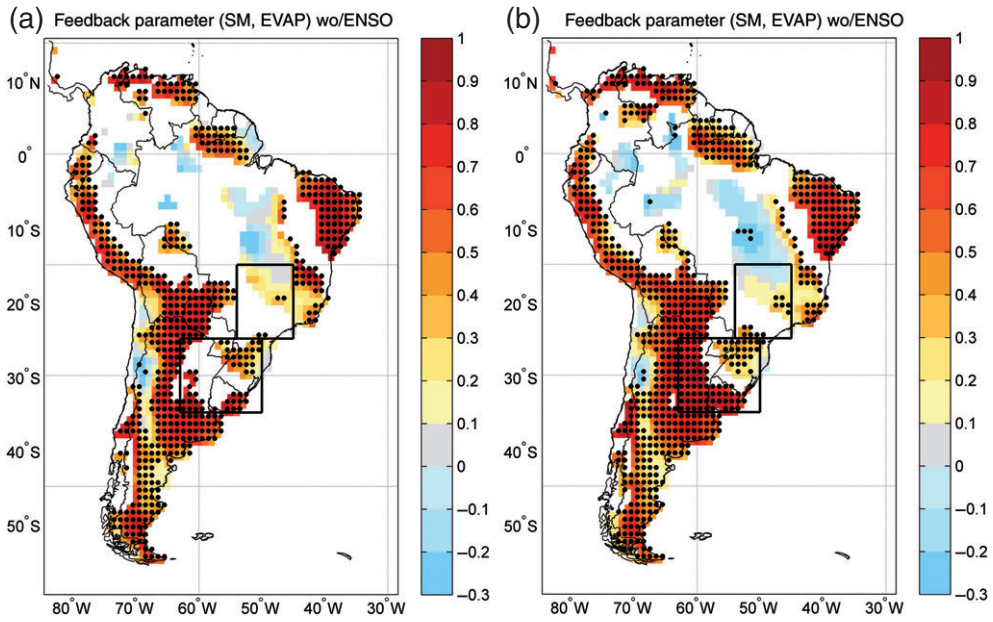

Figure 6. Feedback parameter (λ_{evap}-DJF) for normalized soil moisture–evapotranspiration. Shading appears for simultaneous correlation (at 90% confidence level) between precipitation and evapotranspiration anomalies.

strength between soil moisture and evapotranspiration using, for example, λ_{evap} (Figure 6), but showing only the regions were evapotranspiration and precipitation are positively correlated. According to this analysis, the feedback parameter between soil moisture and evapotranspiration is dominantly positive and is significant (and larger) over regions characterized by moderate to low mean soil moisture and evapotranspiration amounts (see Figure 3), in agreement with the results obtained by Dirmeyer (2011). This is another way to recognize transitional climate regimes, where evapotranspiration is mainly controlled by soil moisture (see Figure 2(a)). Although there are differences between samples with and without ENSO years, they are smaller than in the case of λ_p.

Combining the analysis of λ_p and λ_{evap} for non-ENSO periods, both parameters are positive and significant in the southern tip of the continent and over small areas in Bolivia (particularly in the limits with Brazil, Paraguay and Northern Argentina) and some isolated parts of coastal Brazil and central Argentina. On the other hand, some areas with negative and significant λ_p in SESA, show positive or not significant λ_{evap} values, supporting the hypothesis of increased precipitation through enhanced instability over this region. This would be represented by a reversed example of a NC branch of Figure 2(a) (not sketched in the diagram) starting from soil moisture ↓, evapotranspiration ↓, temperature ↑ resulting in precipitation ↑. This idea is reinforced by the fact that the feedback parameter between soil moisture and 2 m temperature (obtained from GLDAS 2 forcing data set) is negative (not shown) over this particular region. A similar result was obtained by Müller and Seneviratne (2012), analysing lagged correlation of the Standardized Precipitation Index (SPI) (leading), as a proxy of soil moisture, and the number of hot days of the warmest month.

When the sample includes ENSO years, the combined analysis leads to similar conclusions, with stronger signals. Interestingly, the area with positive λ_p around 20°S, 50°W (continental SACZ), that appears in both samples, does not show significant λ_{evap} suggesting that this area is more characterized by an energy limited type of coupling.

A complementary calculation that can be useful to our analysis is the simultaneous correlation between the evapotranspiration and 2 m temperature (Figure 7). Positive correlation values indicate regions under 'atmospheric control' and negative correlation values 'land surface control' (see Figure 2(a) and (b)). This figure also allows us to discern regions of transitional climate over the domain of study. For non-ENSO years, negative or non-significant values over SESA reinforce the idea of prevalent land control while the opposite is observed over portions of SACZ and the southern tip of the continent. When ENSO years are included, the spatial patterns remain similar, but there is an areal enhancement of the negative correlation, mainly over SESA and particularly over Argentina and Uruguay.

As mentioned in the Introduction, we are also interested in evaluating the potential of these diagnostics in the context of monthly and longer scales forecasts: in terms of deriving tools to increase monthly to seasonal forecasts value, strong and significant coupling strength can be used to anticipate increased/decreased precipitation associated with given soil moisture anomalies during the previous month. Of particular relevance for us are the hot spots over eastern Argentina, Uruguay and in the southern tip of the continent, where there are very few predictors for precipitation anomalies particularly for non-ENSO years. Thus, we calculated λ_p and λ_{evap} for each individual month, only for the non-ENSO sample, starting with November precipitation and evapotranspiration. Now, the number of

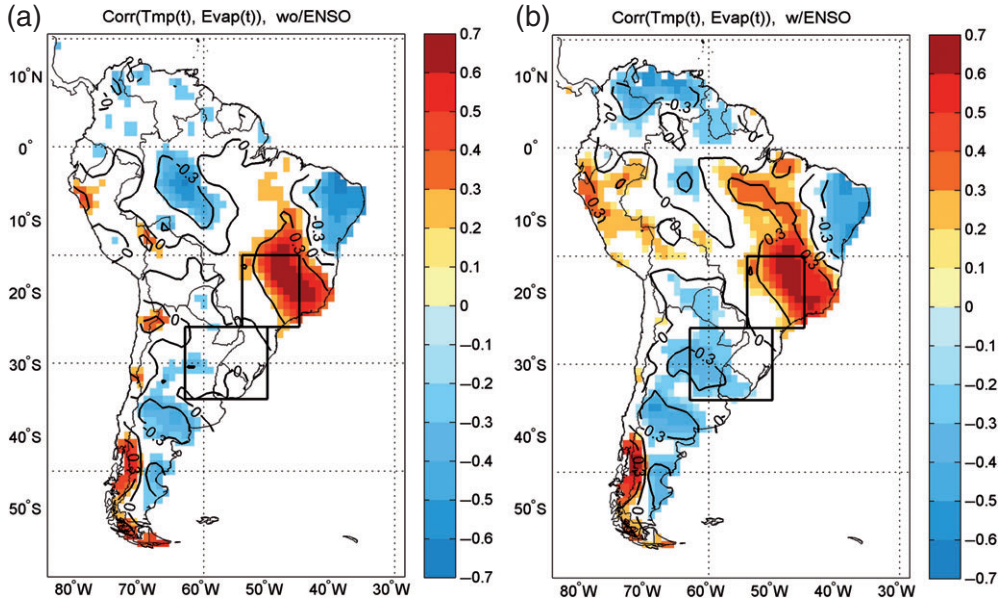

Figure 7. Simultaneous correlation (at 90% confidence level) between 2 m temperature (°C) and evapotranspiration (mm month^{-1}) anomalies for DJF.

months in each sample is smaller (i.e. 19 months in each case), so the robustness of the result might be affected. Still there are very interesting results from this calculation that can be discussed with the aid of Figure 8. At a first glance it is evident that there are different behaviours between individual months that suggest that coupling strength is variable within the same season. In January, λ_p seems to be completely different from the other months, showing large areas characterized by negative values.

Focusing on specific regions, the stronger and more coherent positive coupling with soil moisture over SESA is for December precipitation, although it may not be due to enhanced evaporation, because λ_{evap} for this month is not significant. In turn, there is a λ_p hot-spot in the limit between Bolivia, Paraguay and Argentina that occurs on every month except for January and could be more clearly attributed to the enhanced soil moisture – enhanced evapotranspiration – enhanced precipitation type of coupling.

Monthly changes in λ_{evap} are not as large as in λ_p and sign reversals are rare, except over a small area in the northern boundary of SACZ. In particular, the area of significantly positive λ_p around 20°S, 50°W appears every month (it is reduced in January) but the coupling mechanisms are not directly related with enhanced local evapotranspiration. This result is in correspondence with Grimm *et al.* (2007) findings, who relate enhanced precipitation in January over this area with the development of local circulations that trigger convection and not to enhanced soil moisture/evaporation.

4. Discussion

On the basis of on an off-line simulation of the NOAH LSM, forced by observations and reanalysis from the GLDAS-2 dataset, a statistical methodology has been used to assess land surface–atmosphere coupling strength over South America during the summer season. Evidences of the existence of hot spots between soil moisture and precipitation anomalies have been found. Their location does not match previous works (e.g. Notaro, 2008; Zeng *et al.*, 2010; Dirmeyer, 2011), although they may not be completely comparable due to different sources of data and/or methodologies. The areal extent of these hot spots is larger over tropical regions, where the results should be taken with caution, because this methodology cannot distinguish if precipitation anomalies are linked to remote influences (e.g. related with ENSO signal), to precipitation persistence or to local effects. In order to account for ENSO related feedbacks, ENSO years have been removed from the sample and a comparative analysis of periods with and without ENSO has been undertaken. Results show that physical mechanisms related with possible soil moisture–precipitation interactions vary among the different regions and do not remain the same when ENSO years are eliminated. However, our methodology does not allow to assess whether larger areas with significant λ_p during ENSO years is due to SST interactions with soil moisture and precipitation or just reflect that during ENSO events, interactions between soil moisture and atmosphere are stronger.

Special emphasis has been given to the analysis of two sub-regions, SESA and SACZ, where distinct behaviours have been identified. For instance, central SESA shows significant negative coupling strength ($\lambda_p < 0$) accompanied by not significant λ_{evap}, suggesting that an increase (decrease) of precipitation anomalies related with a decrease (increase) of soil moisture anomalies occurs through an enhancement of atmospheric instability (stability) via augmented (diminished) surface temperature. This is in part corroborated by negative values of soil

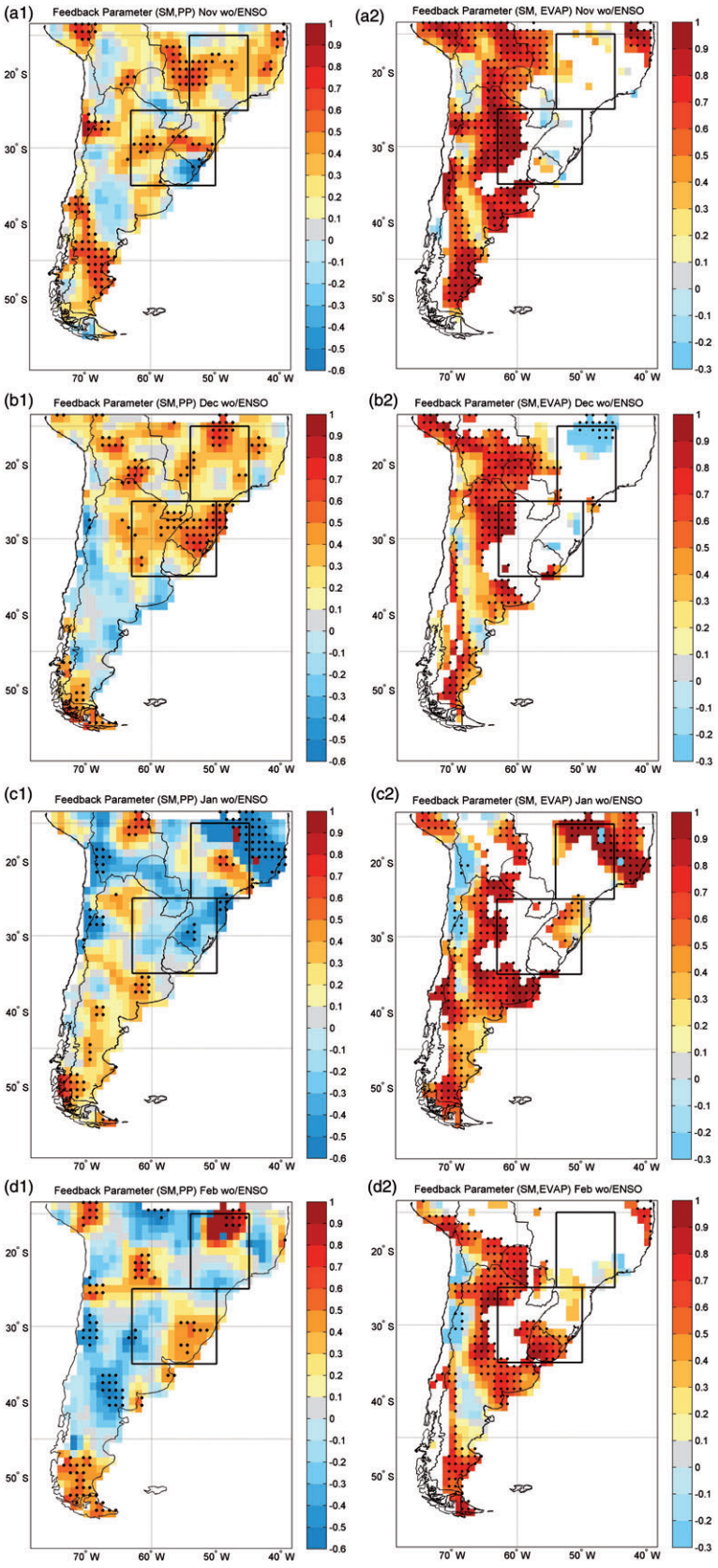

Figure 8. Correlation between monthly mean soil moisture (NDJ) and precipitation (DJF) anomalies (at 90% confidence level, shaded), and soil moisture autocorrelation (lag 1 month, in contours), feedback parameter (λ_p, DJF) for normalized soil moisture-precipitation, without ENSO summers, for November (a1 λ_p, a2 λ_{evap}), December (b1 λ_p, b2 λ_{evap}), January (c1 λ_p, c2 λ_{evap}), and February (d1 λ_p, d2 λ_{evap}).

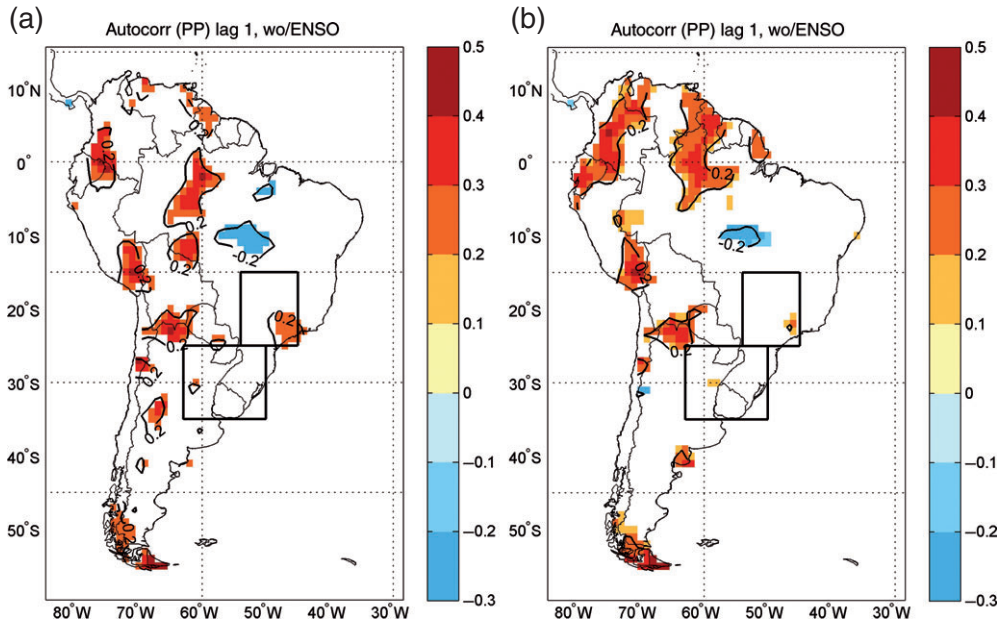

Figure 9. Autocorrelation of November-to-February precipitation anomalies (lag 1 month, 90% confidence level, shaded). Left (a) sample without (b) ENSO summers.

moisture-2 m temperature coupling strength over this region (not shown) and it is also compatible with a land control type of interaction inferred from the correlation between 2 m temperature and evapotranspiration (Figure 7). In turn, the main feature over northeastern SESA is that λ_{evap} has positive and significant values combined with maximum amounts of evapotranspiration. Thus, this part of SESA shows a strong control of soil moisture on evapotranspiration, which is not translated into precipitation anomalies, because λ_p is small and not significant (shows a mix of positive and negative values).

The SACZ region, on the other hand, shows positive and large soil moisture–precipitation feedback parameter, but with no significant soil moisture–evapotranspiration interaction, indicating that this is a region under atmospheric control (or energy limited), supported by positive 2 m temperature–evapotranspiration correlations in this area.

As mentioned in the first section, Sörensson *et al.* (2010)estimated the coupling strength over South America, using GLACE methodology for one austral summer (1992–1993, neutral ENSO conditions). They found over SACZ a mayor soil moisture–precipitation hot spot, but with weak soil moisture–evapotranspiration coupling strength and low evapotranspiration variability. Despite that our study is based on monthly time scales, both methodologies arrive to similar conclusions over the SACZ region. Over SESA, the results on soil moisture/precipitation coupling-strength present opposite signs, although over certain places there is an agreement between the soil moisture–evapotranspiration relations.

Therefore, SESA seems to be a region where the land surface states do exhibit control on the atmosphere that could be plausible in multiple time scales. This is not the case for SACZ. Nevertheless, further studies are still needed to understand different coupling strength signs and the physical mechanisms involved.

When ENSO years are considered, the most important features observed are: a sign reversal of λ_p over SESA; and an enhancement of areas with positive and more intense λ_p particularly in tropical regions. The latter result confirms the considerable impact of ENSO on precipitation over the Tropics, while other areas with significant (and positive) λ_p remain unaffected, such as the hot spots localized in the southern tip of South America and in the limit between Argentina, Bolivia and Paraguay. Here, both λ_p and λ_{evap} are large and appear combined with relatively low values of evapotranspiration, more evident in the southern region. Therefore, the following question arises: How much moisture could be effectively translated into the atmosphere in order to impact precipitation in these areas? As it is discussed by Wei *et al.* (2008), in tropical regions precipitation can have its own memory (besides ENSO). Combined with the fact that precipitation has considerable effect on soil moisture (Guo *et al.*, 2006), lagged covariability between these variables may be, in fact, affected by the precipitation persistence (Wei *et al.*, 2008).

To address this hypothesis, precipitation persistence is analysed in Figure 9. Coincident with many areas with high λ_p (Figure 4), precipitation persistence also shows large positive values, thus suggesting that high correlations between leading soil moisture and precipitation over these regions could in fact be influenced by precipitation persistence, without any substantial contribution of soil moisture. This could be the case over the southern tip of South America, where low evaporation values (Figure 1) are observed. Our results show a hot spot over this region

that resembles the area of strong coupling after removing low frequency variability due to SST in Sun and Wang (2012), although there are differences in the exact location that may be due to their low resolution experiment. This hot spot has not been analysed in detail before and is coincident with a transition zone combining atmospheric–land control regimes, highlighting the regional complexity of the land–atmosphere interactions taking place. This result motivates further analysis over this particular region, to clarify the physical mechanism leading to the precipitation persistence and its interaction with land surface variables.

The seasonal analysis has been complemented by an individual monthly analysis of λ_p and λ_{evap} for the non-ENSO sample. The motivation was to evaluate whether the relationship between soil moisture and precipitation that has been found for the whole season, holds for each individual month. The ultimate goal would be to ascertain the value of a diagnostic based on land–atmospheric coupling in improving climate predictions at monthly time scales. Interestingly, this first assessment clearly shows that the relation between soil moisture and precipitation changes from month to month, and may even reverse its sign over specific regions such as SESA. Moreover, while λ_p over SESA is negative at seasonal scales (Figure 4), it is positive for every month except January (Figure 8). This is an indication that monthly analysis should be performed to serve as a basis for seasonal forecasts.

Land–atmosphere coupling strength analyses have diverse limitations, including the lack of observational data to validate the results, which, in turn, can be largely model dependent, as it is shown in Guo *et al.* (2006) and Koster *et al.* (2006). These authors found that the hot spots location and intensity where model dependent, based on the GLACE experiment. Thus, as GLDAS-2 uses only one Land Surface Model (NOAH) it could be argued that using different LSM, the spatial pattern and intensity of the coupling strength may change. A complementary assessment to show the impact of using different LSMs (see the Appendix), suggests that model dependency does not modify our main results. Although results with GLDAS-1 and GLDAS-2 may not be completely comparable, it is possible that, because both are uncoupled systems, it could be a relatively small impact to LSM choice in our results.

In relation with coupling strength analysis using the NOAH-LSM coupled to the Climate Forecast System, Dirmeyer (2013) found that evaporation is sensitive to soil moisture in transition zones between arid and humid regions, a necessary condition for soil-atmosphere coupling strength. The author also argues that the weak response observed by Zhang *et al.* (2011) may be a result of not considering the surface soil layer of the NOAH LSM in their analysis.

Regarding the GLDAS-2 dataset reliability some basic comparisons done against an observational precipitation data set indicates that this forcing, which might be considered the most important, is well represented at monthly time scales. Yet, alternative data sets should be used to analyse GLDAS-2 (e.g. WATCH) representativeness more in detail. In this sense, as mentioned in Section 3, Müller and Seneviratne (2012) used the SPI, as a proxy for soil moisture, and the number of hot days of the warmest month, in order to analyse the influence of the land surface states on heat waves. Their results over parts of SESA and SACZ are in agreement with ours, showing that both regions have an important land–atmosphere (soil moisture-2 m temperature) coupling strength. In Spennemann *et al.* (2014) an evaluation is carried out, comparing the correspondence between SPI (3 months, derived from observations GPCC, Meyer-Christoffer *et al.*, 2011) against the GLDAS-2 soil moisture. Significant correlations (>0.7) are found over SESA and parts of SACZ, confirming that the GLDAS-2 soil moisture used in this study, has a tied relationship with observed SPI. At some extent, this means that GLDAS-2 soil moisture is a representative quantity of the soil conditions over the region.

The methodology used in this study has some drawbacks: we assume that ENSO is the only external forcing for the precipitation (other external forcing may be still acting); non-linear feedbacks are not taken into account and, probably, the strongest limitation is that it cannot be used to establish a precise causal-effect relationship between the variables under analysis. Nevertheless this simple methodology gives a valuable first order approximation of a highly complex system of land surface–atmosphere interactions that characterize mid-latitude and subtropical areas in South America while showing potential for its application at sub-seasonal forecasts.

Acknowledgements

This work has been funded by the following projects: the Inter-American Institute for Global Change Research (IAI) CRN3035 which is supported by the US National Science Foundation (Grant GEO-1128040), ANPCyT PICT-2010-2110 and UBACyT 20020100100434. The data used in this study were acquired as part of the mission of NASA's Earth Science Division and archived and distributed by the Goddard Earth Sciences (GES) Data and Information Services Center (DISC). The South American Precipitation data (Sa22) was provided by the NOAA/OAR/ESRL PSD, Boulder, Colorado, USA.

Appendix

Figure A1 shows λ_p for different GLDAS-1 LSMs: MOSAIC, VIC, CLM2 and NOAH (see Rodell *et al.*, 2004 for details about each LSM). All LSMs show a similar spatial pattern and coupling strength sign, in agreement with the results shown by Z08 for the northern hemisphere.

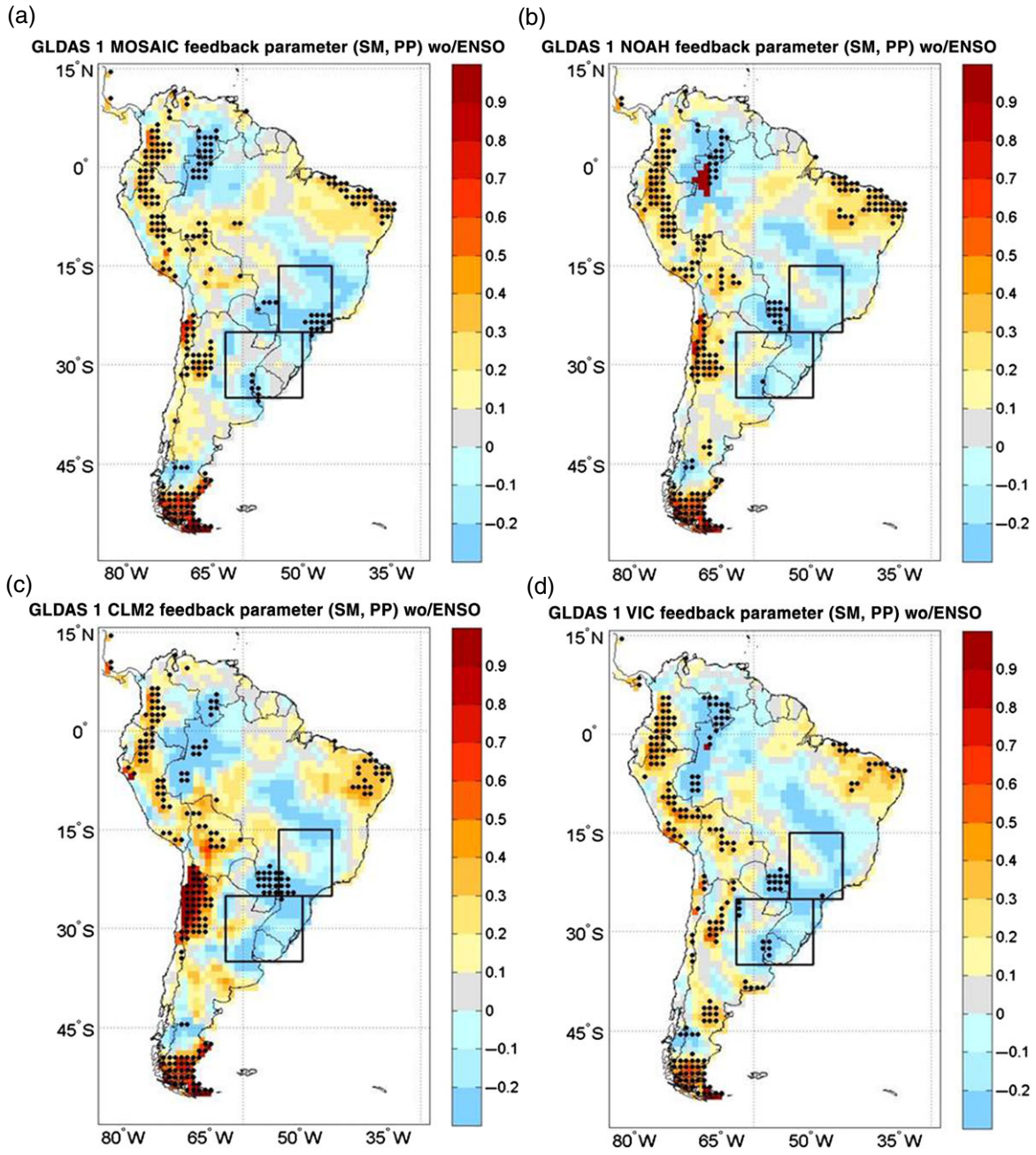

Figure A1. Correlation between monthly mean soil moisture (NDJ) and precipitation (DJF) anomalies (at 90% confidence level, shaded), and soil moisture autocorrelation (lag 1 month, in contours) for GLDAS-1 land surface models: MOSAIC (a), NOAH (b), CLM2 (c) and VIC (d). From 1995 to 1997 were not considered due to technical problems reported by GLDAS-1 data set developers.

The main difference is related with signal significance over some areas.

References

Betts AK. 2009. Land-surface-atmosphere coupling in observations and models. *J. Adv. Model. Earth Syst.* **1**, doi: 10.3894/JAMES.2009.1.4.

Betts AK, Ball JH, Beljaars ACM, Miller MJ, Viterbo P. 1996. The land-surface-atmosphere interaction: a review based on observational and global modeling perspectives. *J. Geophys. Res.* **101**: 7209–7225, doi: 10.1029/95JD02135.

Chen F, Mitchell K, Schaake J, Xue Y, Pan H, Koren V, Duan Y, Ek MB, Betts AK. 1996. Modeling of land-surface evaporation by four schemes and comparison with FIFE observations. *J. Geophys. Res.* **101**(D3): 7251–7268.

Czaja A, Frankignoul C. 2002. Observed impact of Atlantic SST anomalies on the North Atlantic Oscillation. *J. Clim.* **15**: 606–623, doi: 10.1175/1520-0442(2002)015<0606:OIOASA>2.0.CO;2.

Dirmeyer PA. 2011. The terrestrial segment of soil moisture–climate coupling. *Geophys. Res. Lett.* **38**: L16702, doi: 10.1029/2011GL048268.

Dirmeyer PA. 2013. Characteristics of the water cycle and land–atmosphere interactions from a comprehensive reforecast and reanalysis data set: CFSv2. *Clim. Dyn.* **41**: 1083–1097, doi: 10.1007/s00382-013-1866-x.

Dirmeyer PA, Tan L. 2001. A multi-decadal global land-surface data set of state variables and fluxes. COLA Technical Report 102, Center for Ocean-Land-Atmosphere Studies, Calverton, MD, 43 pp.

Dirmeyer PA, Gao X, Zhao M, Guo Z, Oki T, Hanasaki N. 2006. GSWP-2: multimodel analysis and implications for our perception

of the land surface. *Bull. Am. Meteorol. Soc.* **87**: 1381–1397, doi: 10.1175/BAMS-87-10-1381.

Dirmeyer PA, Schlosser CA, Brubaker KL. 2009. Precipitation, recycling, and land memory: an integrated analysis. *J. Hydrometeorol.* **10**: 278–288, doi: 10.1175/2008JHM1016.1.

Ek MB, Mitchell KE, Lin Y, Rogers E, Grunmann P, Koren V, Gayno G, Tarpley JD. 2003. Implementation of Noah land surface model advances in the National Centers for Environmental Prediction operational mesoscale Eta model. *J. Geophys. Res.* **108**(D22): 8851, doi: 10.1029/2002JD003296.

Frankignoul C, Hasselmann K. 1977. Stochastic climate models. Part II: application to sea-surface temperature variability and thermocline variability. *Tellus* **29**: 284–305.

Frankignoul C, Czaja A, L'Heveder B. 1998. Air–sea feedback in the North Atlantic and surface boundary conditions for ocean models. *J. Clim.* **11**: 2310–2324.

Gottschalck J, Meng J, Rodell M, Houser P. 2005. Analysis of multiple precipitation products and preliminary assessment of their impact on global land data assimilation system land surface states. *J. Hydrometeorol.* **6**: 573–598.

Grimm A, Pal J, Giorgi F. 2007. Connection between spring conditions and peak summer monsoon rainfall in South America: role of soil moisture, surface temperature, and topography in Eastern Brazil. *J. Clim.* **20**: 5929–5945.

Guo Z, Dirmeyer PA. 2006. Evaluation of the Second Global Soil Wetness Project soil moisture simulations: 1. Intermodel comparison. *J. Geophys. Res.* **111**: D22S02, doi: 10.1029/2006JD007233.

Guo Z, Dirmeyer PA, Hu ZZ, Gao X, Zhao M. 2006. Evaluation of GSWP-2 soil moisture simulations. Part II: sensitivity to external meteorological forcing. *J. Geophys. Res.* **111**: D22S03, doi: 10.1029/2006JD007845.

Huffman GJ, Adler RF, Morrissey MM, Bolvin DT, Curtis S, Joyce R, McGavock B, Susskind J. 2001. Global precipitation at one-degree daily resolution from multisatellite observations. *J. Hydrometeorol.* **2**: 36–50.

Huffman GJ, Stocker EF, Bolvin DT, Nelkin EJ. 2003. Analysis of TRMM 3-hourly multi-satellite precipitation estimates computed in both real and post-real time. Preprints, *12th Conference on Satellite Meteorology and Oceanography*, American Meteorological Society: Long Beach, CA, CD-ROM, P4.11.

Jaksa WT, Sridhar V, Huntington JL, Khanal M. 2013. Evaluation of the complementary relationship using Noah land surface model and North American Regional Reanalysis (NARR) data to estimate evapotranspiration in semiarid ecosystems. *J. Hydrometeorol.* **14**: 345–359, doi: 10.1175/JHM-D-11-067.1.

Kalnay E, Kanamitsu M, Kistler R, Collins W, Deaven D, Gandin L, Iredell M, Saha S, White G, Woollen J, Zhu Y, Leetmaa A, Reynolds R, Chelliah M, Ebisuzaki W, Higgins W, Janowiak J, Mo KC, Ropelewski C, Wang J, Jenne R, Joseph D. 1996. The NCEP/NCAR 40-year reanalysis project. *Bull. Am. Meteorol. Soc.* **77**: 437–471.

Kato H, Rodell M, Beyrich F, Cleugh H, van Gorsel E, Liu H, Meyers TP. 2007. Sensitivity of land surface simulations to model physics, parameters, and forcings, at four CEOP sites. *J. Meteorol. Soc. Jpn.* **85A**: 187–204.

Koster RD, Dirmeyer PA, Hahmann AN, Ijpelaar R, Tyahla L, Cox P, Suarez MJ. 2002. Comparing the degree of land–atmosphere interaction in four atmospheric general circulation models. *J. Hydrometeorol.* **3**: 363–375.

Koster RD, Dirmeyer PA, Guo Z, Bonan G, Chan E, Cox P, Gordon CT, Kanae S, Kowalczyk E, Lawrence D, Liu P, Lu CH, Malyshev S, McAvaney B, Mitchell K, Mocko D, Oki T, Oleson K, Pitman A, Sud YC, Taylor CM, Verseghy D, Vasic R, Xue Y, Yamada T. 2004. Regions of strong coupling between soil moisture and precipitation. *Science* **305**: 1138–1140, doi: 10.1126/science.1100217.

Koster RD, Guo Z, Dirmeyer PA, Bonan G, Chan E, Cox P, Davies H, Gordon CT, Kanae S, Kowalczyk E, Lawrence D, Liu P, Lu CH, Malyshev S, Mcavaney B, Mitchell K, Mocko D, Oki T, Oleson KW, Pitman A, Sud YC, Taylor CM, Verseghy D, Vasic R, Xue Y, Yamadan T. 2006. GLACE: the global land–atmosphere coupling experiment. Part I: overview. *J. Hydrometeorol.* **7**: 590–610.

Koster RD, Guo Z, Yang R, Dirmeyer PA, Mitchell K, Puma MJ. 2009. On the nature of soil moisture in land surface models. *J. Clim.* **22**(16): 4322–4335, doi: 10.1175/2009JCLI2832.1.

Koster RD, Mahanama SPP, Yamada TJ, Balsamo G, Berg AA, Boisserie M, Dirmeyer PA, Doblas-Reyes FJ, Drewitt G, Gordon CT, Guo Z, Jeong JH, Lawrence DM, Lee WS, Li Z, Luo L, Malyshev S, Merryfield WJ, Seneviratne SI, Stanelle T, van den Hurk BJJM, Vitart F, Wood EF. 2010. Contribution of land surface initialization to subseasonal forecast skill: first results from a multi-model experiment. *Geophys. Res. Lett.* **37**(2): L02402, doi: 10.1029/2009gl041677.

Lee S-J, Berbery EH. 2012. Land cover change effects on the climate of the La Plata Basin. *J. Hydrometeorol.* **13**: 84–102.

Liebmann B, Allured D. 2005. Daily precipitation grids for South America. *Bull. Am. Meteorol. Soc.* **86**: 1567–1570, doi: 10.1175/BAMS-86-11-1567.

Liu Z, Notaro M, Kutzbach J, Liu N. 2006. Assessing global vegetation–climate feedbacks from observations. *J. Clim.* **19**: 787–814.

Livneh B, Xia Y, Mitchell KE, Ek MB, Lettenmaier DP. 2010. Noah LSM snow model diagnostics and enhancements. *J. Hydrometeorol.* **11**: 721–738, doi: 10.1175/2009JHM1174.1.

Marengo JA, Liebmann B, Grimm AM, Misra V, Silva Dias PL, Cavalcanti FA, Carvalho LMV, Berbery EH, Ambrizzi T, Vera CS, Saulo AC, Nogues-Paegle J, Zipser E, Seth A, Alvese LM. 2012. Review: recent developments on the South American monsoon system. *Int. J. Climatol.* **32**: 1–21, doi: 10.1002/joc.2254.

Mei R, Wang GL. 2012. Summer land-atmosphere coupling strength in the United States: comparison among observations, reanalysis data and numerical models. *J. Hydrometeorol.* **13**: 1010–1022, doi: 10.1175/JHM-D-11-075.1.

Meyer-Christoffer A, Becker A, Finger P, Rudolf B, Schneider U, Ziese M. 2011. GPCC climatology version 2011 at 1.0: monthly land-surface precipitation climatology for every month and the total year from rain-gauges built on GTS-based and historic data. 10.5676/DWD_GPCC/CLIM_M_V2011_100, Department of Hydrometeorology, Global Precipitation Climatology Centre, Deutscher Wetterdienst (DWD), Offenbach, Germany. http://www.dwd.de (accessed 23 November 2013).

Mitchell TD, Jones PD. 2005. An improved method of constructing a database of monthly climate observations and associated high-resolution grids. *Int. J. Climatol.* **25**: 693–712, doi: 10.1002/joc.1181.

Müller B, Seneviratne SI. 2012. Hot days induced by precipitation deficits at the global scale. *Proc. Natl. Acad. Sci. U. S. A.* **109**(31): 12398–12403.

Müller OV, Berbery EH, Alcaraz-Segura D, Ek M. 2014. Regional model simulations of the 2008 drought in southern South America using a consistent set of land surface properties. *J. Clim.* **27**: 6754–6778, doi: 10.1175/JCLI-D-13-00463.1.

Nogués-Paegle J, Mo KC. 2002. Linkages between summer rainfall variability over South America and sea surface temperature anomalies. *J. Clim.* **15**: 1389–1407.

Notaro M. 2008. Statistical identification of global hot spots in soil moisture feedbacks among IPCC AR4 models. *J. Geophys. Res.* **113**: D09101, doi: 10.1029/2007JD009199.

Notaro M, Liu Z, Williams JW. 2006. Observed vegetation–climate feedbacks in the United States. *J. Clim.* **19**: 763–786.

Orlowsky B, Seneviratne SI. 2010. Statistical analyses of land–atmosphere feedbacks and their possible pitfalls. *J. Clim.* **23**: 3918–3932, doi: 10.1175/2010JCLI3366.1.

Rodell M, Houser PR, Jambor U, Gottschalck J, Mitchell K, Meng CJ, Arsenault K, Cosgrove B, Radakovich J, Bosilovich M, Entin JK, Walker JP, Lohmann D, Toll D. 2004. The global land data assimilation system. *Bull. Am. Meteorol. Soc.* **85**(3): 381–394.

Rui H. 2012. *Document for the Global Land Data Assimilation System Version 2 (GLDAS-2) products*. http://disc.sci.gsfc.nasa.gov/hydrology/documentation (accessed 15 October 2014).

Salvucci GD, Saleem JA, Kaufmann R. 2002. Investigating soil moisture feedbacks on precipitation with tests of Granger causality. *Adv. Water Resour.* **25**: 1305–1312.

Schaake J, Duan CQ, Koren V, Mitchell KE, Houser PR, Wood EF, Robock A, Lettenmaier DP, Lohmann D, Cosgrove B, Sheffield J, Luo L, Higgins RW, Pinker RT, Tarpley JD. 2004. An intercomparison of soil moisture fields in the North American Land Data Assimilation System (NLDAS). *J. Geophys. Res.* **109**: D01S90, doi: 10.1029/2002JD003309.

Seneviratne SI, Luthi D, Litschi M, Schar C. 2006. Land atmosphere coupling and climate change in Europe. *Nature* **443**: 205–209, doi: 10.1038/nature05095.

Seneviratne SI, Corti T, Davin EL, Hirschi M, Jaeger EB, Lehner I, Orlowsky B, Teuling AJ. 2010. Investigating soil moisture–climate interactions in a changing climate: a review. *Earth-Sci. Rev.* **99**: 125–161.

Spennemann PC, Rivera JA, Saulo AC, Penalba OC. 2014. A comparison of GLDAS soil moisture anomalies against standardized precipitation

index and multi-satellite estimations over South America. *J. Hydrometeorol*, doi: 10.1175/JHM-D-13-0190.1

Sheffield J, Goteti G, Wood EF. 2006. Development of a 50-yr high-resolution global dataset of meteorological forcings for land surface modeling. *J. Clim.* **19**(13): 3088–3111.

Sörensson A, Menéndez CG, Samuelsson P, Willén U, Hansson U. 2010. Soil-precipitation feedbacks during the South American Monsoon as simulated by a regional climate mode. *Clim. Change* **98**: 429–447, doi: 10.1007/s10584-009-9740-x.

Sridhar V, Elliott RL, Chen F. 2003. Scaling effects on modeled surface energy-balance components using the NOAH-OSU land surface model. *J. Hydrol.* **280**(1): 105–123.

Stackhouse PW, Gupta SK, Cox SJ, Mikowitz JC, Zhang T, Chiacchio M. 2004. 12-year surface radiation budget data set. GEWEX News, Vol. 14, No. 4, International GEWEX Project Office, Silver Spring, MD, 10–12.

von Storch H, Zwiers FW. 1999. *Statistical Analysis in Climate Research*. Cambridge University Press: New York, NY, 499 pp.

Sun S, Wang G. 2012. The complexity of using a feedback parameter to quantify the soil moisture-precipitation relationship. *J. Geophys. Res.* **117**: D11113, doi: 10.1029/2011JD017173.

Uppala SM, KÅllberg PW, Simmons AJ, Andrae U, Bechtold VDC, Fiorino M, Gibson JK, Haseler J, Hernandez A, Kelly GA, Li X, Onogi K, Saarinen S, Sokka N, Allan RP, Andersson E, Arpe K, Balmaseda MA, Beljaars ACM, Berg LVD, Bidlot J, Bormann N, Caires S, Chevallier F, Dethof A, Dragosavac M, Fisher M, Fuentes M, Hagemann S, Hólm E, Hoskins BJ, Isaksen L, Janssen PAEM, Jenne R, Mcnally AP, Mahfouf J-F, Morcrette J-J, Rayner NA, Saunders RW, Simon P, Sterl A, Trenberth KE, Untch A, Vasiljevic D, Viterbo P, Woollen J. 2005. The ERA-40 re-analysis. *Q. J. R. Meteorol. Soc.* **131**: 2961–3012, doi: 10.1256/qj.04.176.

Vera CS, Baez J, Douglas M, Emanuel C, Marengo JA, Meitin J, Nicolini M, Nogues-Paegle J, Paegle J, Penalba O, Salio P, Saulo C, Silva Dias MAF, Silva Dias PL, Zipser E. 2006. The South American low-level jet experiment. *Bull. Am. Meteorol. Soc.* **87**: 63–77.

Weedon GP, Gomes S, Viterbo P, Shuttleworth WJ, Blyth E, Österle H, Adam JC, Bellouin N, Boucher O, Best M. 2011. Creation of the WATCH forcing data and its use to assess global and regional reference crop evaporation over land during the twentieth century. *J. Hydrometeorol.* **12**: 823–848, doi: 10.1175/2011JHM1369.1.

Wei J, Dickinson RE, Chen H. 2008. A negative soil moisture–precipitation relationship and its causes. *J. Hydrometeorol.* **9**: 1364–1376, doi: 10.1175/2008JHM955.1.

Xia Y, Ek M, Sheffield J, Livneh B, Huang M, Wei H, Feng S, Luo L, Meng J, Wood E. 2013. Validation of Noah-simulated soil temperature in the North American land data assimilation system phase 2. *J. Appl. Meteorol. Climatol.* **52**(2): 455–471, doi: 10.1175/JAMC-D-12-033.1.

Xia Y, Sheffield J, Ek MB, Dong J, Chaney N, Wei H, Meng J, Wood EF. 2014. Evaluation of multi-model simulated soil moisture in NLDAS-2. *J. Hydrometeorol.* **512**: 107–125, doi: 10.1016/j.jhydrol.2014.02.027.

Zaitchik BF, Rodell M, Olivera F. 2010. Evaluation of the Global Land Data Assimilation System using global river discharge data and a source-to-sink routing scheme. *Water Resour. Res.* **46**: W06507, doi: 10.1029/2009WR007811.

Zeng XB, Barlage M, Castro C, Fling K. 2010. Comparison of land–precipitation coupling strength using observations and models. *J. Hydrometeorol.* **11**: 979–994.

Zhang J, Wang WC, Wei J. 2008. Assessing land-atmosphere coupling using soil moisture from the Global Land Data Assimilation System and observational precipitation. *J. Geophys. Res.* **113**: D17119, doi: 10.1029/2008JD009807.

Zhang L, Dirmeyer PA, Wei J, Guo Z, Lu C. 2011. Land-atmosphere coupling strength in the global forecast system. *J. Hydrometeorol.* **12**(1): 147–156, doi: 10.1175/2010JHM1319.1.

Zhou J, Lau WKM. 2001. Principal modes of interannual and decadal variability of summer rainfall over South America. *Int. J. Climatol.* **21**: 623–1644.

